

sphere, with two acetates not coordinated, or only weakly coordinated, allows considerable distortion to occur. This suggests that the reason the acetates on the Cu(II) complex of TACNTA can be protonated is that there is a stabilization produced by the distortion that occurs. In contrast, for the Ni(II) complex to be protonated would require the sterically efficient acetate group to be replaced by a bulkier water molecule, which would disrupt the tight packing of the donor atoms around the metal ion. In the EDTA complex of Ni(II), in contrast, the packing around the metal ion is not efficient, as the metal ion is considerably too large for the ligand, and thus there is no disruption of an efficiently packed set of donor atoms when an acetate is replaced by a water molecule on protonation of the acetate group.

The  $pK_a$  values and formation constants of the Mg(II) and Ca(II) complexes of TACNTA are seen in Table VII. Also shown are the values for a selection of amine and amino carboxylate ligands. The first  $pK_a$  value for TACNTA is similar to that for 9-aneN<sub>3</sub>, and for other cyclic poly(amino carboxylates) such as DOTA and TETA (Figure 1). What is of particular interest in Table VII is the relative stability of the Ca(II) and Mg(II) complexes as the cavity size of the macrocycle is decreased. In TETA, with its cyclam base fragment to which the acetates are attached, the Ca(II) complex is over 6 orders of magnitude more stable than the Mg(II), while in DOTA with its 12-membered ring this difference has dropped down to a little less than 5. In TACNTA with its nine-membered ring, the progressive decrease in the relative stability of the Ca(II) complex has reached

the point where the Mg(II) complex is now slightly more stable. For both open-chain poly(amino carboxylate) ligands in Table 7, NTA and EDTA, the Ca(II) complex is considerably more stable than that of Mg(II).

The ligand TACNTA shows considerable size selectivity, favoring small metal ions. This leads to stabilization of the small Ni(III) ion to an unusual extent and also a stability for the complex with the small Mg(II) ion, which is unusually high relative to that for the large Ca(II) ion. Of particular interest is the extreme stability of the Ni(II) complex, which we have isolated as a free acid. This unusual stability suggests that the short Ni-N bond lengths observed in the Ni(II) complex of TACNTA do not represent compression, because this should lead to destabilization. Rather, it appears that this shortening of the Ni-N bond is due to the highly efficient packing of TACNTA around the metal ion, which also accounts for the high stability of the complex.

**Acknowledgment.** We thank the Senate Research Committee of the University of the Witwatersrand and the Council for Scientific and Industrial Research for generous financial support. We thank the Technikon (Pretoria) for granting sabbatical leave to M.J.v.d.M. and J. Albain for carrying out the data collection.

**Registry No.** I, 87306-49-8; II, 95250-82-1; TACNTA, 56491-86-2.

**Supplementary Material Available:** Tables of observed and calculated structure factors, anisotropic thermal parameters, and fractional atomic coordinates for hydrogen atoms (12 pages). Ordering information is given on any current masthead page.

Contribution from the Department of Chemistry,  
The University of Michigan, Ann Arbor, Michigan 48109

## Synthesis, Structure, and Fluxional Behavior of 7-Coordinate Complexes: $TpMo(CO)_3X$ ( $X = H, Br, I$ ; $Tp =$ Hydridotripyrazolylborato)

M. DAVID CURTIS\* and KOM-BEI SHIU

Received August 8, 1984

The halogens Br<sub>2</sub> and I<sub>2</sub> react with  $TpMo(CO)_3^-$  ( $Tp =$  hydridotripyrazolylborato) to give the 7-coordinate complexes  $TpMo(CO)_3X$ . The infrared spectra of these complexes, and of  $TpMo(CO)_3H$ , are consistent with a 3:4 (four-legged piano stool) structure both in the solid state and in solution. This is confirmed by the solid-state structure of  $TpMo(CO)_3Br$ :  $a, b, c = 8.305(1), 12.032(1), 8.570(2)$  Å;  $\alpha, \beta, \gamma = 104.39(1), 93.42(1), 92.03(1)^\circ$ ;  $V = 826.9(2)$  Å<sup>3</sup>, space group  $P\bar{1}$ ,  $Z = 2$ . The structure was refined with all non-H atoms anisotropic to conventional agreement indices  $R_1, R_2 = 0.036, 0.058$  based on 1902 reflections with  $I > 3\sigma(I)$ . The structure may be viewed as a 3:4 piano stool or as a distorted capped trigonal prism with Br capping a quadrilateral face. The <sup>1</sup>H and <sup>13</sup>C NMR spectra of  $TpMo(CO)_3X$  ( $X = H, Br, I$ ) show dynamic  $C_{3v}$  symmetry down to -80 °C. This behavior is interpreted in light of EHMO calculations on 3:4 and 3:3:1 (capped octahedron) isomers.

### Introduction

Hydridotripyrazolylborate ( $Tp = HB(C_3H_3N_2)_3^-$ ) complexes of molybdenum show many similarities to their cyclopentadienyl (Cp) analogues.<sup>1</sup> However, one difference in behavior is particularly noteworthy: in contrast to the numerous 7-coordinate cyclopentadienyl complexes of the general type  $CpML_4$ ,<sup>2</sup> very few such derivatives have been reported for the  $Tp$  complexes. These latter are  $TpMo(CO)_3H$ ,  $TpMo(CO)_3Me$ ,  $TpMo(CO)_3Et$ ,<sup>3</sup>  $TpW(CO)_2(CS)I$ ,<sup>4</sup> and the recently reported  $TpTaMe_3Cl$ .<sup>5</sup> Even here, however, we have recently shown that the reported alkyl derivatives are in fact the 6-coordinate  $\eta^2$ -acyl complexes  $TpMo(CO)_2(\eta^2-COR)$ .<sup>6</sup> Although the 7-coordinate alkyl com-

plexes are probably intermediates in the formation of the  $\eta^2$ -acyl complexes from  $TpMo(CO)_3^-$  and alkyl halides, these rearrange spontaneously to the 6-coordinate  $\eta^2$ -acyls.<sup>7</sup> Such facile alkyl migrations, which are not observed in  $CpMo(CO)_3R$  chemistry,<sup>8</sup> were ascribed to the steric and electronic requirements of the  $Tp$  ligand.<sup>6,9</sup>

Thus,  $TpMo(CO)_3H$  is left as the only authentic 7-coordinate  $Tp-Mo$  complex, and this hydride also exhibits different behavior when compared to the  $CpMo(CO)_3H$  hydride. The latter is a weak acid, and its corresponding base,  $CpMo(CO)_3^-$ , may be protonated with weak acids, e.g. acetic acid.<sup>10</sup> Furthermore, the hydrogen may be removed as a hydride by strong Lewis acids,

- (1) (a) Trofimenko, S. *Acc. Chem. Res.* **1971**, *4*, 17. (b) Trofimenko, S. *Chem. Rev.* **1972**, *72*, 497. (c) Shaver, A. J. *J. Organomet. Chem. Libr.* **1977**, *3*, 157.
- (2) Davis, R.; Kane-Maguire, L. A. P. In "Comprehensive Organometallic Chemistry"; Pergamon Press: Oxford, England, 1982; Vol. 3, pp 1177-1199.
- (3) Trofimenko, S. *J. Am. Chem. Soc.* **1969**, *91*, 588.
- (4) Greaves, W. W.; Angelici, R. J. *J. Organomet. Chem.* **1980**, *191*, 49.
- (5) Reger, D. L.; Swift, C. A.; Lebiada, L. *Inorg. Chem.* **1984**, *23*, 349.
- (6) Curtis, M. D.; Shiu, K.-B.; Butler, W. M. *Organometallics* **1983**, *2*, 1475.

- (7) The  $TpMo(CO)_3^-$  anion reacts with arenediazonium ions,  $ArN_2^+$ , to give  $\eta^2$ -aroyl complexes via a free-radical mechanism: (a) Desmond, T.; Lalor, F. J.; Ferguson, G.; Ruhl, B.; Parvez, M. *J. Chem. Soc., Chem. Commun.* **1980**, 55. (b) Desmond, T.; Lalor, F. J.; Ferguson, G.; Parvez, M. *Ibid.* **1983**, 457.
- (8) (a) Wojcicki, A. *Adv. Organomet. Chem.* **1973**, *11*, 87. (b) Calderazzo, F. *Angew. Chem., Int. Ed. Engl.* **1977**, *16*, 229. (c) King, R. B. *Acc. Chem. Res.* **1970**, *3*, 417.
- (9) Shiu, K.-B.; Curtis, M. D.; Huffman, J. C. *Organometallics* **1983**, *2*, 936.
- (10) Piper, T. S.; Wilkinson, G. *J. Inorg. Nucl. Chem.* **1956**, *3*, 104.

e.g.  $\text{Ph}_3\text{C}^+$ .<sup>11</sup> We find that the hydride,  $\text{TpMo}(\text{CO})_3\text{H}$ , does not react with  $\text{Ph}_3\text{CBF}_4$ <sup>12</sup> and that the anion,  $\text{TpMo}(\text{CO})_3^-$ , appears to be a weaker base than  $\text{CpMo}(\text{CO})_3^-$ . Thus, strong acid, e.g. HCl, is required to fully protonate the  $\text{TpMo}(\text{CO})_3^-$  anion under conditions where acetic acid suffices to protonate  $\text{CpMo}(\text{CO})_3^-$ . Also, when it is dissolved in polar but weakly basic solvents, e.g. DMF, the IR spectrum of solutions of  $\text{TpMo}(\text{CO})_3\text{H}$  clearly show the presence of the anion,  $\text{TpMo}(\text{CO})_3^-$ , presumably resulting from the acid-base dissociation of the Mo-H bond. These observations taken together suggest that  $\text{TpMo}(\text{CO})_3\text{H}$  is more protonic and less hydridic than the cyclopentadienyl analogue,  $\text{CpMo}(\text{CO})_3\text{H}$ . This conclusion is somewhat unexpected since the  $\text{Tp}^-$  ligand is a better electron donor than  $\text{Cp}^-$  as judged from the lower  $\nu_{\text{CO}}$  frequencies in  $\text{TpMo}(\text{CO})_3^-$  vs.  $\text{CpMo}(\text{CO})_3^-$ .<sup>3</sup> Therefore, we conclude that the 7-coordinate  $\text{TpMo}(\text{CO})_3\text{H}$  complex is more destabilized with respect to its 6-coordinated anion than is the case in the cyclopentadienyl system. In other words, the  $\text{Tp}$  ligand appears to polarize the metal orbitals into an octahedral array much more efficiently than does the delocalized charge of the  $\text{Cp}$  anion.

These considerations led us to attempt the preparation of further examples of 7-coordinate  $\text{TpMo}$  complexes. Of particular interest to us was the possibility of observing a capped octahedral (3:3:1) structure (A) for  $\text{TpMoL}_4$  complexes since Kubaček et al.<sup>13</sup> have calculated that such a 3:3:1 structure represents a minimum in the potential energy surface for  $\text{CpML}_4$  complexes whose global minimum (ground state) is always the "four-legged piano stool" or 3:4 structure (B).



We report here the synthesis of the new 7-coordinate complexes  $\text{TpMo}(\text{CO})_3\text{X}$  ( $\text{X} = \text{Br}$ , I), the structure of the bromide, and the fluxionality of these halides and  $\text{TpMo}(\text{CO})_3\text{H}$ . We have also performed a EHMO study of  $\text{TpMo}(\text{CO})_3\text{Br}$ , and these results are compared to those reported for  $\text{CpMo}(\text{CO})_3\text{X}$ .<sup>13</sup> The structure of  $\text{TpMo}(\text{CO})_3\text{Br}$  was communicated in preliminary form.<sup>6</sup>

### Experimental Section

**General Information.** All operations were carried out under a  $\text{N}_2$  atmosphere by using standard Schlenk techniques or in an inert-atmosphere box with a recirculating purification train. Solvents MeOH, MeCN,  $\text{CH}_2\text{Cl}_2$ , and hexane were dried (4A Molecular Sieves for the former two,  $\text{P}_2\text{O}_5$  for the latter), and distilled under  $\text{N}_2$  prior to use. NaTp was prepared by the published procedure.<sup>14</sup> Elemental analyses were performed by Galbraith or Schwarzkopf Microanalytical Laboratories. Melting points were obtained with a Thomas-Hoover apparatus with samples sealed in evacuated or  $\text{N}_2$ -filled capillaries.  $^1\text{H}$  NMR spectra were recorded on Varian T-60A or Bruker WM-360 spectrometers.  $^{13}\text{C}$  NMR spectra were recorded on the Bruker WM-360 at 90.56 MHz. IR spectra were obtained on a Perkin-Elmer 1330 grating instrument and calibrated with polystyrene film. The B-H stretching mode of all neutral  $\text{Tp}$  complexes is close to  $2500\text{ cm}^{-1}$ .

**Tetraethylammonium Tricarbonyl(hydridotripyrazolylborato)molybdate(0),  $[\text{Et}_4\text{N}][\text{TpMo}(\text{CO})_3]$ .** The original procedure for this salt was modified as follows: A mixture of 0.94 g (4.0 mmol) of NaTp and 1.06 g (4.02 mmol) of  $\text{Mo}(\text{CO})_6$  in 150 mL of acetonitrile was stirred at reflux until 300 mL of gas was evolved. A deaerated solution of 1.20 g of  $\text{Et}_4\text{NBr}$  in 100 mL of  $\text{H}_2\text{O}$  then was added to the yellow-green reaction mixture to give yellow crystals. These were collected and washed two times with 5 mL of  $\text{CH}_2\text{Cl}_2$  and once with 5 mL of hexane and then dried under vacuum; yield 1.90 g (90%). The compound melts at  $284^\circ\text{C}$  dec. IR (KBr): 1890 (s), 1750 (vs)  $\text{cm}^{-1}$ .  $^1\text{H}$  NMR (30  $^\circ\text{C}$ ,  $\text{CD}_3\text{CN}$ , 60 MHz):  $\delta$  6.70 (d,  $\text{H}_3$ , 3 H), 6.65 (d,  $\text{H}_5$ , 3 H), 5.13 (t,  $\text{H}_4$ , 3 H) ( $^3J_{\text{H}_3,\text{H}_4}$ ,

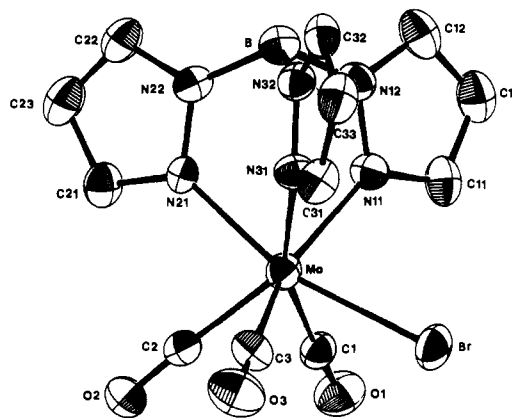


**Figure 1.** ORTEP plot of  $\text{TpMo}(\text{CO})_3\text{Br}$  ( $\text{Tp} =$  hydridotripyrazolylborate), with numbering scheme, emphasizing the 3:4 structure (50% probability ellipsoids).

$\approx ^3J_{\text{H}_3,\text{H}_4} \approx 2\text{ Hz}$ ), 3.06 (q,  $\text{CH}_2$ , 8 H), 1.15 (tt,  $\text{CH}_3$ , 12 H), 2.10 (s, BH).

**Bromotricarbonyl(hydridotripyrazolylborato)molybdenum(II),  $\text{TpMo}(\text{CO})_3\text{Br}$ .** A suspension of  $[\text{Et}_4\text{N}][\text{TpMo}(\text{CO})_3]$  (5.78 g, 11.0 mmol) in 30 mL of  $\text{CH}_2\text{Cl}_2$  was treated dropwise with a solution of  $\text{Br}_2$  (0.57 mL of  $\text{Br}_2$  in 25 mL of  $\text{CH}_2\text{Cl}_2$ ) at room temperature. After the addition of  $\text{Br}_2$  was complete, 30 mL of MeOH was added to give a dark yellow precipitate. This solid was collected and recrystallized from  $\text{CH}_2\text{Cl}_2$ /hexane to give 4.68 g (90%) of product, mp  $115^\circ\text{C}$  dec. Anal. Calcd for  $\text{C}_{12}\text{H}_{10}\text{BBrMoN}_6\text{O}_3$ : C, 30.48; H, 2.13. Found: C, 30.29; H, 2.17. IR (KBr): 2047 (s), 1970 (s), 1935 (s)  $\text{cm}^{-1}$ . IR ( $\text{CH}_2\text{Cl}_2$ ): 2053 (s), 1980 (s), 1938 (s)  $\text{cm}^{-1}$ .  $^1\text{H}$  NMR (30  $^\circ\text{C}$ , acetone- $d_6$ , 360 MHz):  $\delta$  6.40 (t,  $\text{H}_4$ , 3 H), 5.60 (d,  $\text{H}_3$ , 3 H), 5.32 (d,  $\text{H}_5$ , 3H), ( $^3J_{\text{H}_3,\text{H}_4} = 2.2$ ,  $^3J_{\text{H}_4,\text{H}_5} = 2.1\text{ Hz}$ ).  $^{13}\text{C}\{^1\text{H}\}$  NMR (+30 to  $-80^\circ\text{C}$ ,  $\text{CD}_2\text{Cl}_2$ ):  $\delta$  144 ( $\text{C}_3$ ), 135 ( $\text{C}_5$ ), 105 ( $\text{C}_4$ ), 228 (CO).

**Iodotricarbonyl(hydridotripyrazolylborato)molybdenum(II),  $\text{TpMo}(\text{CO})_3\text{I}$ .** **1. Preparation.** Iodine (2.00 g, 7.88 mmol) was added portionwise to 45 mL of  $\text{CH}_3\text{CN}$  in which was dissolved 3.30 g (6.31 mmol) of  $[\text{Et}_4\text{N}][\text{TpMo}(\text{CO})_3]$ . The mixture was stirred at  $25^\circ\text{C}$  for 20 min. Filtration of the mixture gave an orange-red solid, which was washed with 10 mL of hexane and then dried under vacuum to yield 3.05 g (93%) of product, mp  $180^\circ\text{C}$  dec. This product is normally obtained pure, but if necessary it may be recrystallized from  $\text{CH}_2\text{Cl}_2$ /hexane. Anal. Calcd for  $\text{C}_{12}\text{H}_{10}\text{BIMoN}_6\text{O}_3$ : C, 27.72; H, 1.94. Found: C, 27.91; H, 2.00. IR (KBr): 2016 (s), 1950 (s), 1910 (s)  $\text{cm}^{-1}$ . IR (THF): 2020 (s), 1955 (s), 1922 (s)  $\text{cm}^{-1}$ .  $^1\text{H}$  NMR (30  $^\circ\text{C}$ , acetone- $d_6$ , 60 MHz):  $\delta$  6.25 (t,  $\text{H}_4$ , 3 H), 7.78 (d,  $\text{H}_5$ , 3 H), 8.16 (d,  $\text{H}_3$ , 3 H) ( $^3J_{\text{H}_3,\text{H}_4} \approx ^3J_{\text{H}_4,\text{H}_5} \approx 2\text{ Hz}$ ).  $^{13}\text{C}\{\text{gated-}^1\text{H}\}$  NMR (30  $^\circ\text{C}$ ,  $\text{CDCl}_3$ ):  $\delta$  146 (d,  $\text{C}_3$ ,  $J = 190\text{ Hz}$ ), 135 (d,  $\text{C}_5$ ,  $J = 190\text{ Hz}$ ), 106 (d,  $\text{C}_4$ ,  $J = 195\text{ Hz}$ ), 237 (s, CO).

**2. Pyrolysis.**  $\text{TpMo}(\text{CO})_3\text{I}$  (2.20 g, 4.23 mmol) was pyrolyzed in 150 mL of refluxing MeCN. Gas evolution was observed but not quantitated. After gas evolution ceased (ca. 85 min), a solution IR spectrum was obtained that indicated the formation of the triply bonded dimer,  $\text{Tp}_2\text{Mo}_2(\text{CO})_4$ .<sup>9</sup> The solvent was then stripped off under vacuum, and 10 mL of  $\text{CH}_2\text{Cl}_2$  was added to the residue. This suspension was then filtered and the solid washed two times with 5 mL of  $\text{CH}_2\text{Cl}_2$ . The combined filtrate and washings were concentrated to a volume of ca. 3 mL to give 0.6 g (39%, based on total Mo) of green, crystalline  $\text{Tp}_2\text{Mo}_2(\text{CO})_4$ .

**Hydridotricarbonyl(hydridotripyrazolylborato)molybdenum(II),  $\text{TpMo}(\text{CO})_3\text{H}$ .** The preparation of this compound was modified from the original procedure<sup>3</sup> as follows: A 1-mL aliquot of concentrated aqueous HCl (12 M) was added dropwise to 25 mL of a solution of  $[\text{Et}_4\text{N}][\text{TpMo}(\text{CO})_3]$  (0.86 g, 1.64 mmol) in MeCN with rapid stirring. A light yellow precipitate formed immediately. Filtration gave 0.56 g (86%) of product, mp  $209\text{--}211^\circ\text{C}$ . IR ( $\text{CH}_2\text{Cl}_2$ ): 2008 (s), 1910 (s), 1890 (sh)  $\text{cm}^{-1}$ . IR (THF): 2000 (s), 1906 (s), 1887 (s)  $\text{cm}^{-1}$ .  $^1\text{H}$  NMR (30  $^\circ\text{C}$ , acetone- $d_6$ , 360 MHz):  $\delta$  6.31 (t,  $\text{H}_4$ , 3 H), 5.72 (d,  $\text{H}_3$ , 3 H), 5.48 (d,  $\text{H}_5$ , 3 H) ( $^3J_{\text{H}_3,\text{H}_4} = 2.4$ ,  $^3J_{\text{H}_4,\text{H}_5} = 1.9\text{ Hz}$ ),  $-3.02$  (s, MoH, 1 H).  $^{13}\text{C}\{\text{gated-}^1\text{H}\}$  NMR (30  $^\circ\text{C}$ ,  $\text{CDCl}_3$ ):  $\delta$  145 (d,  $\text{C}_3$ ,  $J = 186\text{ Hz}$ ), 135 (d,  $\text{C}_5$ ,  $J = 187\text{ Hz}$ ), 106 (d,  $\text{C}_4$ ,  $J = 178\text{ Hz}$ ), 221 (d, CO,  $^2J_{\text{CH}} = 3\text{ Hz}$ ).

**X-ray Structure Determination of  $\text{TpMo}(\text{CO})_3\text{Br}$ .** Crystals of this complex, grown from  $\text{CH}_2\text{Cl}_2$ /hexane at room temperature, consisted of two types: dark yellow, thick plates and paler yellow, thin needles. Crystals of both types were examined on the diffractometer and were found to be identical in their crystallographic parameters. A crystal with the chunkier habit was used to collect the data (Syntex  $\text{P}_2$  diffractometer,  $22 \pm 2^\circ\text{C}$ ).

(11) Beck, W.; Schleiter, K. *Z. Naturforsch. B: Anorg. Chem., Org. Chem.* **1978**, *33*, 1214.

(12) Shiu, K.-B. Ph.D. Thesis, The University of Michigan, 1984.

(13) Kubaček, P.; Hoffmann, R.; Halvas, Z. *Organometallics* **1982**, *1*, 180.

(14) Trofimenko, S. *J. Am. Chem. Soc.* **1967**, *89*, 3170.

Table I. Crystal Data for  $\text{TpMo}(\text{CO})_3\text{Br}$ 

fw	472.90 ( $\text{C}_{12}\text{H}_{10}\text{BBrMoN}_6\text{O}_3$ )
color	dark yellow
radiation	Mo $\text{K}\alpha$
$\rho_{\text{calcd}}/\text{g mL}^{-1}$	1.899
$\rho_{\text{found}}/\text{g mL}^{-1}$	1.89 (flotation method, MeI/MeOH)
cell dimens	
$a, b, c/\text{Å}$	8.305 (1), 12.032 (1), 8.570 (2)
$\alpha, \beta, \gamma/\text{deg}$	104.39 (1), 93.42 (1), 92.03 (1)
$V/\text{Å}^3$	826.9 (2)
space group	$P\bar{1}$ (No. 2), triclinic
$Z$	2
std reflns	(301), (06 $\bar{1}$ ), (1 $\bar{1}$ 3)
$2\theta_{\text{max}}/\text{deg}$	45
cryst dimens, mm	0.13 × 0.21 × 0.21
$\mu/\text{cm}^{-1}$	31.897
transmission factors (max, min)	0.66, 0.56
total no. of reflns	2305 ( $h, \pm k, \pm l$ )
no. of reflns with $I > 3\sigma(I)$ (NO)	1902
no. of variables	217
$R_1, R_2^a$	0.036, 0.058
$[\Sigma w( F_o  -  F_c )^2 / (\text{NO} - \text{NV})]^{1/2}$	2.31

<sup>a</sup>  $R_1 = \Sigma |F_o| - |F_c| / \Sigma |F_o|$ ,  $R_2 = [\Sigma w(|F_o| - |F_c|)^2 / \Sigma w F_o^2]^{1/2}$ , and  $w = 4F_o^2 / [\sigma^2(F_o^2) + (0.04F_o^2)^2]$ .

Table II. Fractional Atomic Coordinates

atom	$x$	$y$	$z$
Mo	0.0951 (1)	0.24474 (5)	0.4232 (1)
Br	0.3787 (1)	0.2449 (1)	0.2958 (1)
C1	0.0870 (8)	0.3728 (6)	0.3146 (8)
C2	-0.1015 (9)	0.2210 (6)	0.2787 (8)
C3	0.0966 (9)	0.0991 (7)	0.2493 (9)
O1	0.0848 (7)	0.4486 (5)	0.2565 (6)
O2	-0.2132 (6)	0.2084 (5)	0.1880 (6)
O3	0.1017 (8)	0.0150 (5)	0.1550 (7)
N11	0.2082 (7)	0.3787 (4)	0.6317 (6)
N21	-0.0996 (6)	0.2620 (4)	0.5917 (6)
N31	0.1875 (7)	0.1287 (5)	0.5707 (6)
N12	0.1971 (7)	0.3713 (5)	0.7860 (7)
N22	-0.0674 (7)	0.2633 (5)	0.7504 (6)
N32	0.1871 (7)	0.1594 (5)	0.7353 (7)
C11	0.3035 (9)	0.4728 (6)	0.6389 (9)
C21	-0.2610 (8)	0.2712 (6)	0.5728 (9)
C31	0.2788 (9)	0.0368 (6)	0.5337 (9)
C13	0.352 (1)	0.5266 (7)	0.800 (1)
C23	-0.330 (1)	0.2783 (7)	0.719 (1)
C33	0.3404 (9)	0.0106 (6)	0.673 (1)
C12	0.2849 (9)	0.4591 (6)	0.892 (1)
C22	-0.2053 (9)	0.2726 (6)	0.8266 (9)
C32	0.2798 (8)	0.0887 (6)	0.7995 (9)
B	0.106 (1)	0.2663 (7)	0.823 (1)

Table IV. Bond Distances (Å) in  $\text{TpMo}(\text{CO})_3\text{Br}$ 

	$n = 1$	$n = 2$	$n = 3$	av
Mo-Cn	1.987 (7)	1.957 (7)	1.999 (8)	1.982 ± 0.016
Mo-Nn1	2.222 (5)	2.213 (5)	2.231 (5)	2.222 ± 0.006
Nn1-Nn2	1.356 (7)	1.367 (7)	1.366 (7)	1.363 ± 0.004
Nn1-Cn1	1.344 (9)	1.353 (8)	1.345 (8)	1.347 ± 0.004
Cn1-Cn3	1.399 (11)	1.394 (10)	1.383 (11)	1.392 ± 0.006
Cn3-Cn2	1.391 (11)	1.358 (11)	1.380 (10)	1.376 ± 0.007
Cn2-Nn2	1.364 (9)	1.347 (9)	1.359 (8)	1.357 ± 0.006
Nn2-B	1.558 (9)	1.531 (10)	1.522 (10)	1.537 ± 0.014
Cn-On	1.143 (9)	1.155 (8)	1.131 (8)	1.143 ± 0.008
Mo-Br	2.655 (1)			

The structure was solved by a combination of Patterson and Fourier difference maps. Table I lists the crystallographic statistics and Table II the fractional atomic coordinates; the derived bond distances and angles are collected in Tables IV and V, respectively. Figure 1 is an ORTEP plot of the molecule with complete numbering scheme, and Figure 2 is a view of the inner coordination sphere along the Mo→B axis. See the paragraph at the end of the paper concerning supplementary material. Programs used in the data reduction and refinement are described in ref

Table V. Bond Angles (deg) in  $\text{TpMo}(\text{CO})_3\text{Br}$ 

C1-Mo-C2	71.7 (3)	C1-Mo-C3	107.0 (3)
C2-Mo-C3	68.5 (3)	N21-Mo-N31	81.8 (2)
N11-Mo-N21	79.4 (2)	N11-Mo-N31	82.0 (2)
C1-Mo-N11	84.0 (2)	C2-Mo-N21	77.0 (2)
C3-Mo-N31	80.7 (3)	C1-Mo-N21	108.8 (2)
C1-Mo-N31	160.6 (2)	C2-Mo-N11	138.2 (3)
C2-Mo-N31	127.4 (3)	C3-Mo-N11	153.1 (3)
C3-Mo-N21	118.0 (3)	C1-Mo-Br	76.0 (2)
C2-Mo-Br	118.5 (2)	C3-Mo-Br	73.2 (2)
N11-Mo-Br	86.3 (1)	N21-Mo-Br	164.3 (1)
N31-Mo-Br	89.1 (1)	N12-B-N22	106.5 (6)
N12-B-N32	107.0 (6)	N22-B-N32	109.1 (6)
C11-N11-Mo	131.6 (5)	C21-N21-Mo	133.0 (5)
C31-N31-Mo	131.4 (5)	N12-N11-Mo	121.8 (4)
N22-N21-Mo	121.2 (4)	N32-N31-Mo	120.9 (4)
N12-N11-C11	106.5 (6)	N22-N21-C21	105.8 (5)
N32-N31-C31	106.3 (5)	N11-C11-C13	110.0 (7)
N21-C21-C23	109.9 (7)	N31-C31-C33	110.3 (7)
C11-C13-C12	106.1 (7)	C21-C23-C22	105.7 (7)
C31-C33-C32	106.0 (6)	C13-C12-N12	106.4 (7)
C23-C22-N22	108.8 (7)	C33-C32-N32	107.5 (6)
C12-N12-B	127.9 (6)	C22-N22-B	128.4 (6)
C32-N32-B	128.3 (6)	N11-N12-B	120.8 (5)
N21-N22-B	121.5 (5)	N31-N32-B	121.5 (5)
Mo-C1-O1	177.9 (7)	Mo-C2-O2	176.7 (6)
Mo-C3-O3	177.2 (7)		

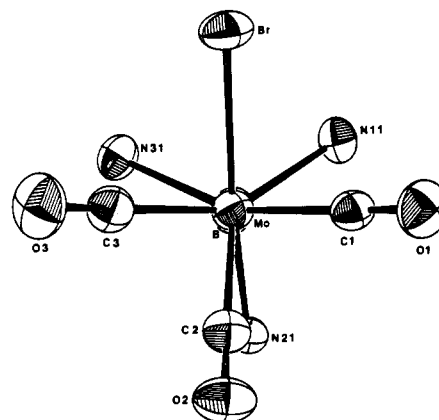


Figure 2. ORTEP plot of the inner coordination sphere of  $\text{TpMo}(\text{CO})_3\text{Br}$  (viewed along the Mo→B axis) emphasizing the capped-trigonal-prism description (Br caps the quadrilateral face) (50% probability ellipsoids).

15. Neutral-atom scattering factors for all non-hydrogen atoms were taken from Cromer and Mann,<sup>16</sup> while those for hydrogen atoms are from Stewart, Davidson, and Simpson.<sup>17</sup> The real and imaginary components of anomalous dispersion for Mo and Br were applied to the calculated structure factors by use of the values of Cromer.<sup>18</sup>

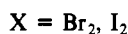
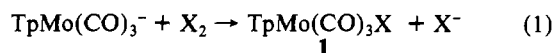
**EHMO Calculations.** The calculations were performed with Hoffmann's programs, ICONS and FMO with the "weighted  $H_{ij}$ " option.<sup>19</sup> The atomic parameters are given in ref 13 except those for Br which were as follows ( $n_l, H_{ij}$  (eV),  $f$ ): 4s, -25.0, 2.64; 4p, -14.0, 2.26. The  $\text{TpMo}$  fragment was assumed to have strict  $C_{3v}$  symmetry with bond distances and angles as found for  $\text{TpMo}(\text{CO})_3$ .<sup>9</sup> The M-C-O angles were all set at  $180^\circ$ , all C-H and B-H distances were set at 1.0 Å, and other distances were as follows (Å): Mo-N, 2.21; Mo-CO, 1.98; C-O, 1.16; B-N, 1.36; C-N, 1.54; C-C, 1.38. The energy minimum for the 3:3:1 ( $C_{3v}$ ) structure was obtained by keeping the  $\text{TpMo}$  fragment fixed and

- (15) All calculations were carried out on an Amdahl 470 computer at the University of Michigan Computing Center. Programs used during the structure analysis were SYNCOR (data reduction by W. Schmonsees), FORDAP (Fourier synthesis by A. Zalkin), ORFLS (full-matrix least-squares refinement by Busing, Martin, and Levy), ORFFE (distances, angles, and their esd's by Busing, Martin, and Levy), ORTEP (thermal ellipsoid plots by C. K. Johnson), and PLANES (least-squares planes by D. M. Blow).
- (16) Cromer, D. T.; Mann, J. B. *Acta Crystallogr., Sect. A* **1968**, *A24*, 321.
- (17) Stewart, R. F.; Davidson, E. R.; Simpson, W. T. *J. Chem. Phys.* **1965**, *42*, 3175.
- (18) Cromer, D. T. *Acta Crystallogr.* **1965**, *18*, 17.
- (19) Ammeter, J. H.; Burgi, H.-B.; Thibeault, J. C.; Hoffmann, R. *J. Am. Chem. Soc.* **1978**, *100*, 3686.

varying the Br–Mo–CO angle while  $C_{3v}$  symmetry was maintained. The actual structure of the 3:4 isomer was idealized to strict  $C_3$  symmetry. A second 3:4 isomer was investigated that differed from the observed structure by a rotation of the Tp group about the Mo–Br axis by  $60^\circ$  (this eclipses the Mo–Br bond with one pz ring).

### Results and Discussion

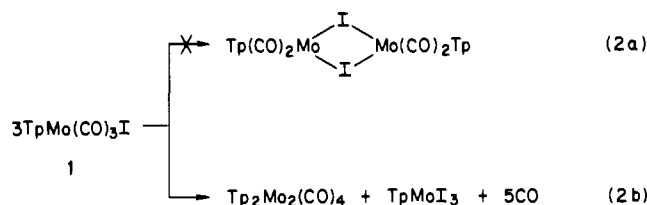
**Synthesis and Properties of  $TpMo(CO)_3X$ .** The halides ( $X = Br, I$ ) are readily prepared by the reaction of the appropriate halogen with the anion,  $TpMo(CO)_3^-$  (eq 1). These complexes



are yellow ( $X = Br$ ) to orange-red ( $X = I$ ) and are sparingly soluble in most organic solvents with the exception of  $CH_2Cl_2$  and  $CH_3CN$ . As solids, the halides may be handled in air, but in solution, slow decomposition occurs. The air-sensitive hydride ( $X = H$ ) was prepared previously by addition of strong acid to the anion.<sup>3</sup> All three of these 7-coordinate complexes display three  $\nu_{CO}$  bands in the IR spectra as befits a complex with  $C_3$  symmetry ( $2A' + A''$ ). These bands are observed both in the solid state and in solution.

The  $\nu_{CO}$  frequencies of the Tp derivatives are generally 10–20  $cm^{-1}$  lower than those of the corresponding Cp complexes.<sup>10,20</sup> This observation suggests that Tp is a better electron donor than Cp. The charges on Mo (calculated by the EHMO method) also support this conclusion. The calculated charges on Mo are 0.26+ and 0.12– in the neutral radicals  $CpMo(CO)_3$  and  $TpMo(CO)_3$ , respectively. Interestingly, the increased negative charge on Mo is not passed on to the carbonyls according to the calculations: 0.15 e is transferred from the CpMo fragment to the  $(CO)_3$  fragment as compared to a transfer of 0.14 e from the TpMo fragment. Undoubtedly, a charge-iterated calculation would show a greater charge transfer for the TpMo fragment, but both the calculations and experiment<sup>21</sup> suggest that the Tp ligand is a slightly better  $\pi$ -acceptor than Cp and thus competes with the carbonyls for metal  $\pi$  electrons.

We have previously shown that mild thermolysis of the paramagnetic tricarbonyl  $TpMo(CO)_3$  gives a quantitative conversion to the triply bonded dimer,  $Tp_2Mo_2(CO)_4$  ( $M \equiv Mo$ ).<sup>9</sup> This facile loss of CO suggested that thermolysis of the iodo derivative (**1**) would give the complex  $Tp_2(CO)_4Mo_2(\mu-I)_2$  (eq 2a), a complex



analogous to that obtained by the reaction of  $I_2$  with  $Cp_2Mo_2(CO)_4$  ( $M \equiv Mo$ ).<sup>22</sup> However, in refluxing MeCN, complex **1** ( $X = I$ ) undergoes a disproportionation to give an 86% yield of  $Tp_2Mo_2(CO)_4$  according to the stoichiometry in eq 2b.

**Structure of  $TpMo(CO)_3Br$ .** The molecular structure of  $TpMo(CO)_3Br$  may be described as a version of the "four-legged piano stool" (or 3:4) structure commonly found for  $CpMoL_4$  complexes (Figure 1). There is no crystallographically imposed symmetry, but the molecule closely approximates  $C_3$  symmetry with the mirror plane containing one carbonyl (C2O2), the N22-pyrazolyl (pz) ring, and the Mo, Br, and Br atoms (Figure 2).

(20) Hart-Davis, A. J.; White, C.; Mawby, R. J. *Inorg. Chim. Acta* **1970**, *4*, 431.

(21) The  $^1H$  NMR spectrum of the paramagnetic complex  $TpMo(CO)_3$  shows that the odd electron is delocalized onto the Tp ligand almost exclusively by  $\pi$ -bonding: Curtis, M. D.; Shiu, K.-B., submitted for publication.

(22) Curtis, M. D.; Fotinos, N. A.; Han, K. R.; Butler, W. M. *J. Am. Chem. Soc.* **1983**, *105*, 2686.

Table VII. Comparison of Selected Angles (deg) in  $LMO(CO)_3X$

L	X	trans	trans	cis	ref
		OC–M–X	OC–M–CO	OC–M–CO	
Cp	Cl	136.8 <sup>a</sup>	107.0 <sup>a</sup>	74.8, 78.6	23
Cp	$CH_2CO_2H$	131.9	108.8	76.4, 77.7	24
Cp	$C_3F_7$	131.9	116.9	75.4, 77.3	25
[9]aneN <sub>3</sub> <sup>b</sup>	Br	126.4	104.9	69.9, 75.3	26
Tp	Br	118.5	107.0	68.5, 71.7	

<sup>a</sup> Calculated from the atomic positions given in ref 23.

<sup>b</sup> [9]aneN<sub>3</sub> = 1,4,7-triazacyclononane. This complex is a cation.

Some structural features of the  $Mo(CO)_3X$  portion of  $CpMo(CO)_3Cl$ ,<sup>23</sup>  $CpMo(CO)_3CH_2CO_2H$ ,<sup>24</sup>  $CpMo(CO)_3CF_2CF_2CF_3$ ,<sup>25</sup>  $([9]aneN_3)Mo(CO)_3Br^+$  ( $[9]aneN_3 = 1,4,7$ -triazacyclononane),<sup>26</sup> and  $TpMo(CO)_3Br$  are compared in Table VII. For the Cp complexes, the average value for the trans OC–M–X angle is  $134 \pm 3^\circ$ , which is considerably larger than this angle in  $TpMo(CO)_3Br$  ( $118.5^\circ$ ) and in  $([9]aneN_3)Mo(CO)_3Br$  ( $126.4^\circ$ ). In the last two structures, the large Br atom occupies a site between two N donor atoms but this arrangement forces the trans carbonyl to lie almost directly under the remaining N-donor ligand (see Figure 2). The steric interactions of the trans carbonyl with a bulky pz ring of the Tp ligand depresses the trans OC–M–X angle. This interaction is present, but to a lesser degree, in the less sterically congested [9]aneN<sub>3</sub> complex. The steric congestion caused by the large Tp and [9]aneN<sub>3</sub> ligands also causes a general constriction of all the angles in the  $Mo(CO)_3X$  portion of the molecule, but the effect is greatest for the trans OC–M–X angle.

The average Mo–N distances in the series  $TpMo(CO)_3Br$ ,  $TpMo(CO)_2(\eta^7-COMe)$ ,<sup>6</sup>  $Tp_2Mo_2(CO)_4$ ,<sup>9</sup>  $TpMo(CO)_3$ ,<sup>9</sup> and  $TpMo(CO)_2NO$ <sup>27</sup> are 2.222 [6], 2.21 [3], 2.22 [3], 2.207 (7), and 2.213 [4] Å. The formal oxidation states of the Mo in this series are +2, +2, +1, +1, and 0. Thus, there is no trend of the Mo–N distance with formal oxidation state in the range +2 to 0. In fact, the variances in Mo–N distances *within* a given complex are often greater than the differences between complexes. For example, the Mo–N21 distance (trans to Br) is slightly shorter than the other two Mo–N distances in  $TpMo(CO)_3Br$ : 2.213 (5) vs. 2.222 (5) and 2.231 (5) Å. We regard these variations in Mo–N distances as a manifestation of the trans influence in these 3:4 piano stool structures. The long Mo–N distances are nearly trans to the carbonyls, which have a high trans influence compared to that of the bromine ligand. Similar trans influences in Mo–C(Cp) distances are also observed in  $CpM(CO)_2L_2$  and  $CpMo(CO)_3L$  complexes.<sup>22,28</sup>

The Mo–Br and Mo–C bond distances are unexceptional and agree well with those reported for other 7-coordinate Mo complexes.<sup>26,29–31</sup>

The structures of  $TpMo(CO)_3Br$  and  $([9]aneN_3)Mo(CO)_3Br^+$  have been described as 3:4 piano stool structures, thus emphasizing their relationship to  $CpML_4$  complexes.<sup>26</sup> However these structures also may be described fairly well as capped trigonal prisms. Such a description of these structures brings them into the mainstream of 7-coordinate complexes, for which three structures have been found to be most commonly adopted. These three structures are the capped trigonal prism ( $C_{2v}$ ), the capped octahedron ( $C_{3v}$ ), and the pentagonal bipyramid ( $D_{5h}$ ).<sup>32,33</sup>

(23) Chaiwasie, S.; Fenn, R. H. *Acta Crystallogr., Sect. B* **1968**, *B24*, 525.

(24) Ariyaratne, J. K. P.; Bierrum, A. M.; Green, M. L. H.; Ishaq, M.; Prout, C. K.; Swanwick, M. G. *J. Chem. Soc. A* **1969**, 1309.

(25) Churchill, M. R.; Fennessey, J. P. *Inorg. Chem.* **1967**, *6*, 1213.

(26) Chaudhuri, P.; Wiegardt, K.; Tsai, Y.-H.; Krüger, C. *Inorg. Chem.* **1984**, *23*, 427.

(27) Holt, E. M.; Holt, S. L.; Cavalito, F.; Watson, K. J. *Acta Chem. Scand., Ser. A* **1976**, *A30*, 225.

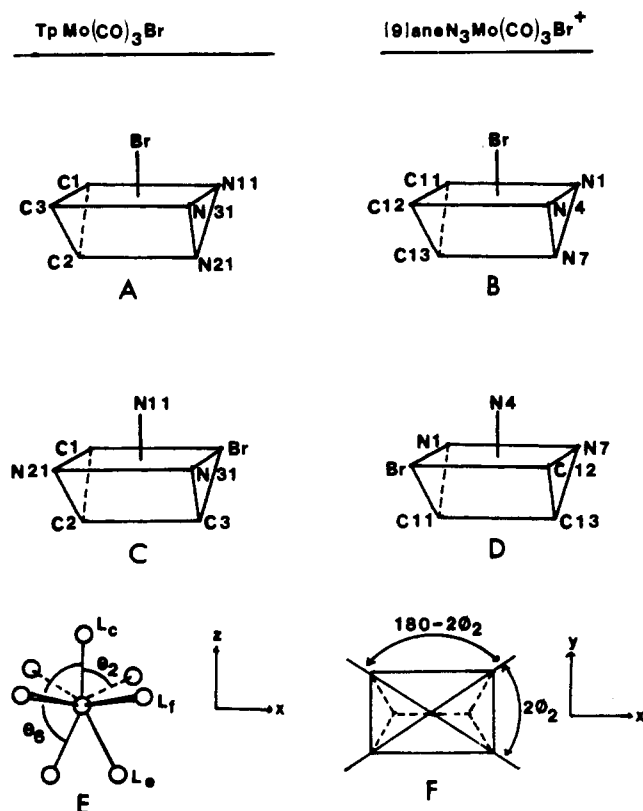
(28) Curtis, M. D.; Han, K. R. *Inorg. Chem.* **1985**, *24*, 378.

(29) Drew, M. G. B. *Prog. Inorg. Chem.* **1977**, *23*, 67.

(30) Drew, M. G. B.; Brisdon, B. J.; Day, A. *J. Chem. Soc., Dalton Trans.* **1981**, 1310.

(31) Elder, M.; Kettle, S. F. A.; Tso, T. C. *J. Crystallogr. Spectrosc. Res.* **1982**, *12*, 65.

Chart I



Due to distortions, two sets of atoms may be used to define the capped trigonal prism in the  $\text{N}_3\text{Mo}(\text{CO})_3\text{Br}$  complexes. These are shown in structures A–D (the atom labeling for the  $[\text{9]aneN}_3$  complex is taken from ref 26) in Chart I. The angles used to describe an ideal capped trigonal prism in which all M–L distances are equal are defined in E and F.<sup>32,33</sup>

In the case at hand,  $\theta_2$  will be taken as the average value of the four  $\text{L}_c\text{--Mo--L}_f$  bond angles where  $\text{L}_c$  is the capping ligand and  $\text{L}_f$  are ligands in the capped, rectangular face.  $\theta_6$  is the angle  $\text{L}_c\text{--Mo--L}_e$  where  $\text{L}_e$  are the two ligands in the unique edge of the capped prism. Strictly,  $\phi_2$  is the angle between the x axis and the plane defined by the z axis unit vector and the M– $\text{L}_c$  vector (see Chart I). Here,  $\phi_2$  was identified with the  $\text{L}_f\text{ML}_f'$  bond angles, giving four values for  $\phi_2$ , which were then averaged.<sup>34</sup> These angles for the various capped prisms, A–D, are collected in Table VIII where they are compared with their "ideal" values.<sup>32,33</sup> Also listed in Table VIII are the angles between several of the planes that define the capped trigonal prism.

As can be seen from Table VIII, both A and C have average values for the angles  $\theta_2$ ,  $\theta_6$ , and  $\phi_2$  that are consistent with their description as idealized, capped trigonal prisms. In C, the Mo–N11 vector is more nearly perpendicular to the plane of the capped face, but A has the advantage in that the best  $\pi$ -donor (Br) is in the capping position in accord with the theoretical predictions of Hoffmann et al.<sup>32</sup> According to their analysis, the better  $\pi$ -donor prefers the capping position and  $\pi$ -acceptors prefer positions in the capped face and unique edge. Accordingly, we prefer description A over C.

For the  $[\text{9]aneN}_3$  complex, description B is preferred over D on the basis of angles  $A_2$ – $A_4$  and the fact that B again has the bromide in the capping position.

Table VIII. Coordination Geometries of  $\text{TpMo}(\text{CO})_3\text{Br}$  and  $([\text{9]aneN}_3)\text{Mo}(\text{CO})_3\text{Br}^+$ , Viewed as Capped Trigonal Prisms

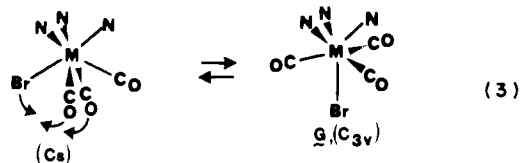
structure	$\theta_2^a$	$\theta_6^a$	$\phi_2^a$	$A_1^b$	$A_2^b$	$A_3^b$	$A_4^b$
A	81	141	48	8.8	90.0	95.8	95.8
B	82	142	46	8.4	92.9	99.3	97.8
C	83	146	48	2.8	85.8	84.7	85.4
D	81	145	52	7.2	84.0	76.5	79.4
ideal <sup>c</sup>	82	148	46–48	0.0	90.0	90.0	90.0

<sup>a</sup> These angles (deg) are defined in Chart I. <sup>b</sup>  $A_i$  = angle (deg) between the M– $\text{L}_c$  vector and the normal to the plane of the capped face ( $\text{P}_1$ ),  $A_2 = \angle \text{P}_1\text{P}_2$ ,  $A_3 = \angle \text{P}_2\text{P}_3$ ,  $A_4 = \angle \text{P}_3\text{P}_4$ . The planes,  $\text{P}_i$ , are defined as follows:  $\text{P}_1 = \text{Mo}, \text{C}1, \text{C}3, \text{N}11, \text{N}31$ ;  $\text{P}_2 = \text{Mo}, \text{Br}, \text{N}21, \text{C}2$ ;  $\text{P}_3 = \text{C}1, \text{C}2, \text{C}3$ ;  $\text{P}_4 = \text{N}11, \text{N}21, \text{N}31$ . <sup>c</sup> Ideal  $\text{C}_{2v}$  capped trigonal prism with all M–L distances equal.<sup>32,33</sup>

**Fluxionality of  $\text{TpMo}(\text{CO})_3\text{X}$  ( $\text{X} = \text{H}, \text{Br}, \text{I}$ ).** 7-Coordinate complexes are notorious for their fluxional behavior in solution. None of the idealized geometries, capped prism (CTP), capped octahedron (COh), or pentagonal bipyramid (PBP), nor any of the less symmetrical arrangements are characterized by a markedly lower total energy.<sup>32,33</sup> Hence, interconversions between these various structures are quite facile. It is not surprising, then, that  $\text{TpMo}(\text{CO})_3\text{X}$  ( $\text{X} = \text{H}, \text{Br}, \text{I}$ ) exhibit fluxional behavior in solution.

These three complexes all exhibit three  $\nu_{\text{CO}}$  bands in their IR spectra. This pattern is consistent with the approximate  $\text{C}_3$  symmetry found for  $\text{TpMo}(\text{CO})_3\text{Br}$  in the solid state, which requires three normal modes ( $2\text{A}' + \text{A}''$ ) involving carbonyl stretching. We thus conclude that all three complexes have essentially the same structure in solution and in the solid state. However, from room temperature to  $-80^\circ\text{C}$ , all these complexes show one set of equivalent pyrazolyl rings and one set of equivalent carbonyl groups in the  $^1\text{H}$  and  $^{13}\text{C}$  NMR spectra. The NMR experiment thus sees dynamic  $\text{C}_{3v}$  structures for  $\text{TpMo}(\text{CO})_3\text{X}$ . In contrast,  $\text{CpMo}(\text{CO})_3\text{X}$  ( $\text{X} = \text{Cl}, \text{Br}, \text{I}$ ) all show two carbonyl resonances (2:1 ratio) in their  $^{13}\text{C}$  NMR spectra at room temperature.<sup>35,36</sup> Thus, the barrier for interconversion of ligands in the basal plane of the 3:4 structure is much lower in the Tp complexes than in the Cp complexes.

Hoffmann et al.<sup>32</sup> have shown how a minimal motion converts the CTP into a COh geometry. However, it appears that in the case of the  $\text{TpMo}(\text{CO})_3\text{X}$  complexes, such rearrangements alone cannot account for the fluxional process observed here. In this minimal-motion mechanism, five steps are required to convert a capping ligand in the CTP geometry into a capping ligand in the COh geometry ( $\text{X}_{\text{CTP}} \rightarrow \text{uf} \rightarrow \text{cf} \rightarrow \text{e} \rightarrow \text{X}_{\text{COh}}$ , where  $\text{X}_{\text{CTP,COh}}$  = capping ligands in CTP or COh, uf and cf = uncapped and capped faces in COh, and e = ligands in the quadrilateral face and edge of the CTP). Furthermore, the isomers needed to achieve the required averaging to  $\text{C}_{3v}$  symmetry are prohibited by the small bite of the Tp ligand. Therefore, the most plausible intermediate in the observed fluxional process is the 3:3:1 capped octahedron (G) arrived at in one step from the 3:4 isomer (eq 3).



The mechanism shown in eq 3 is similar to the one proposed for the cis–cis (racemization) and cis–trans isomerization of  $\text{CpMo}(\text{CO})_2\text{LX}$  complexes.<sup>37,38</sup> In their elegant study, Fallor

(32) Hoffmann, R.; Beier, B. F.; Muetterties, E. L.; Rossi, A. R. *Inorg. Chem.* **1977**, *16*, 511.

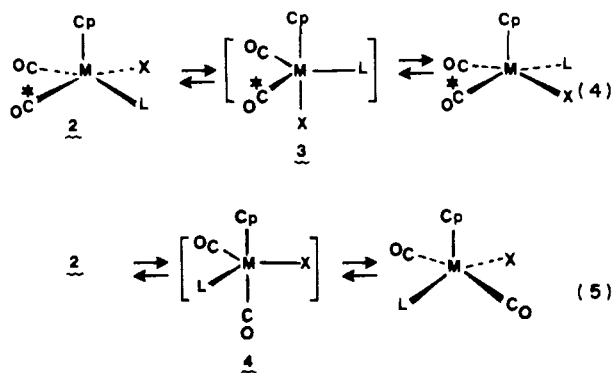
(33) Thompson, H. B.; Bartell, L. S. *Inorg. Chem.* **1968**, *7*, 488.

(34) The use of bond angles rather than angles between planes is justified since (a) the  $\text{L}_f\text{ML}_f'$  bond angles are close to the angles between the planes containing the bonds (the Mo atom is only 0.2 Å out of the plane of the  $\text{L}_f$  ligands) and (b) the individual variations in the value of  $\phi_2$  are greater than the error introduced by using the bond angles for  $\phi_2$ .

(35) Todd, L. J.; Wilkinson, J. R.; Hickey, J. P.; Beach, D. L.; Barnett, K. W. *J. Organomet. Chem.* **1978**, *154*, 151.

(36)  $\text{CpMo}(\text{CO})_3\text{Me}$  shows  $\text{C}_3$  symmetry in the  $^{13}\text{C}$  NMR spectrum at room temperature, but  $(\eta^5\text{-C}_5\text{H}_4\text{CH}_2\text{CH}_2)\text{Mo}(\text{CO})_3$  shows nonequivalent carbonyls at  $-45^\circ\text{C}$  that become averaged at room temperature. The lowering of the energy barrier in the latter complex was attributed to ring strain: Braun, S.; Dahler, P.; Eilbrecht, P. *J. Organomet. Chem.* **1978**, *146*, 135.

et al. showed that the cis-cis barriers were dependent on the halide in  $\text{CpMo}(\text{CO})_2\text{LX}$  but the cis-trans barriers were not.<sup>37,38</sup> In all cases, the activation energy for the cis-cis racemization, which proceeds through intermediate 3, was lower than that for the cis-trans isomerization going through intermediate 4 (eq 4, 5).



Hence, the 3:3:1 intermediate with X in the axial, or capping, position is a few kcal/mol lower in energy than the 3:3:1 isomer with carbonyl in the capping position. The observed activation energies for the cis-trans isomerization for 2 (X = Cl, Br, I; L =  $\text{PR}_3$ ,  $\text{P}(\text{OR})_3$ ) were all in the range of 22–24 kcal/mol. These values compare well with the EHMO results of Kubaček et al.,<sup>13</sup> who calculated that the 3:3:1 structure (3) for  $\text{CpMo}(\text{CO})_3\text{Cl}$  is ca. 24 kcal/mol higher in energy than the 3:4 structure. The latter authors also stated that the 3:3:1 structure is stabilized relative to the 3:4 structure when X is a small ligand with good  $\sigma$ - and  $\pi$ -donor properties.

Since our results from the temperature dependence of the NMR spectra of  $\text{TpMo}(\text{CO})_3\text{X}$  suggest a much lower barrier ( $E_a < 8$  kcal/mol)<sup>39</sup> for this complex, we have carried out some EHMO calculations for various isomers of  $\text{TpMo}(\text{CO})_3\text{Br}$ . These results are collected in Table IX.

Structure I is the observed structure idealized to  $C_s$  symmetry by averaging the related bond angles. In all the structures, the Tp ligand was kept rigid with local  $C_{3v}$  symmetry and equal Mo-N bond lengths (2.21 Å), and all Mo-CO distances were kept fixed at 1.98 Å. Within these constraints, the results incorrectly predict the 3:3:1 structure with an axial carbonyl, J, to have the lowest total energy. The  $C_{3v}$  3:3:1 structure with Br on the axis is predicted to lie only 4.6 kcal/mol above the "observed" structure. The main point here is that the calculations do show that the energy difference between the 3:4 structure (I) and various 3:3:1 structures is expected to be quite small—much smaller than the energy differences between these isomers in the  $\text{CpMo}(\text{CO})_3\text{X}$  complexes. Thus, the 3:3:1 isomers of  $\text{TpMo}(\text{CO})_3\text{X}$  are viable intermediates in the observed fluxional process.

Interconversions between I and J could cause rapid scrambling of the carbonyl groups but would not average the environments of the pz rings. Therefore, the Tp group would also have to rotate with respect to the basal ligands. Several geometries were investigated; they are all 20–25 kcal/mol higher in energy than I. A barrier of this magnitude would be readily measured by NMR.<sup>40</sup> Therefore, we conclude that structure G is the intermediate responsible for averaging the Tp groups, although structure J may contribute to scrambling the carbonyls.

The final question we might address is as follows: "Why is the behavior of  $\text{TpMo}(\text{CO})_3\text{X}$  complexes so different in detail from

Table IX. Total Energies Computed by the EHMO Method for Various Isomers of  $\text{TpMo}(\text{CO})_3\text{Br}^a$

Structure <sup>b</sup>	(C) (deg)	$E_T$ (kcal/mole)
	$\zeta_1 = 53.2$	+24.2
	$\zeta_2 = 53.5$	
	$\zeta_3 = 11.5$	
	$\zeta_4 = 50.0$	
	$\zeta_1 = 71.5$	+ 4.6
	$\zeta_2 = 71.5$	
	$\zeta_1 = 53.2$	(0.0)
	$\zeta_2 = 53.5$	
	$\zeta_3 = 11.5$	
	$\zeta_4 = 65.5$	
	$\zeta_1 = 0.0$	- 6.2
	$\zeta_2 = 71.5$	
	$\zeta_3 = 56.0$	
	$\zeta_4 = 75.0$	

(a) Relative to isomer, I. (b) All structures have  $C_s$  symmetry except G which has  $C_{3v}$  symmetry. (c) The angles  $\zeta$  are measured from the -z axis to the following vectors:  $\zeta_1$ , unique M-CO bond;  $\zeta_2$ , remaining M-CO bonds;  $\zeta_3$ , bisector of the OC-M-CO angle;  $\zeta_4$ , Mo-Br bond. The angle between the z-axis and the Tp-nitrogen atoms was fixed at 49.9°.

the corresponding Cp complexes?" We believe the answer to this is intimately connected to the propensity of  $\text{TpMo}^{\text{II}}$  complexes to be 6-coordinate. As pointed out in the introduction, 7-coordination is the rule for  $\text{CpML}_4$  complexes, but coordination number 6 predominates for  $\text{TpMo}^{\text{II}}$ . It appears as if the localized bonding of the three N donors of the Tp ligand efficiently polarizes the metal orbitals into an octahedral array. The more delocalized  $e'$  donor MO of Cp is less efficient in this respect.

The EHMO results for the fragments  $\text{TpMo}^-$  and  $\text{CpMo}^-$  lend some support for this assertion. The frontier acceptor orbitals of the  $\text{TpMo}^-$  fragment consist of hybrid d orbitals mixed with metal p orbitals to give a set of hybrids strongly polarized away from the N donors. The corresponding orbitals of the  $\text{CpMo}^-$  fragment are pure  $xz$  or  $yz$ , polarized to a lesser extent with  $p_x$  or  $p_y$ , respectively. Both fragments have a comparable  $sp_2$ -hybrid acceptor orbital at higher energy.

Therefore, we believe that the 3:3:1 (COh) structure more closely resembles an octahedral array than the 3:4 (CTP) structure and "fits" more closely the hybridized orbitals of the TpMo fragment. Thus, in  $\text{TpMo}(\text{CO})_3\text{X}$ , the 3:3:1 structure is stabilized with respect to the 3:4 structure and a lower barrier for interconversions between them is observed.

**Acknowledgment.** The authors thank the National Science Foundation (Grant No. CHE-83-05235) for support of this work. K.-B.S. also thanks the Department of Chemistry and the donors for a James E. Harris Fellowship and the Rackham Graduate School and the donors for an Ethyl Corp. Fellowship. We also thank Dr. W. M. Butler for collecting the X-ray data.

**Registry No.**  $[\text{Et}_4\text{N}][\text{TpMo}(\text{CO})_3]$ , 16970-22-2;  $\text{Mo}(\text{CO})_6$ , 13939-06-5;  $\text{TpMo}(\text{CO})_3\text{Br}$ , 86822-13-1;  $\text{Br}_2$ , 7726-95-6;  $\text{TpMo}(\text{CO})_3\text{I}$ , 95156-35-7;  $\text{I}_2$ , 7553-56-2;  $\text{Tp}_2\text{Mo}_2(\text{CO})_4$ , 85803-19-6;  $\text{TpMo}(\text{CO})_3\text{H}$ , 95156-34-6.

**Supplementary Material Available:** Table III (thermal parameters,  $B_{ij}$ ), Table VI (equations of least-squares planes), and Table X (listing of  $F_o$  vs.  $F_c$ ) (12 pages). Ordering information is given on any current masthead page.

(37) Faller, J. W.; Anderson, A. S. *J. Am. Chem. Soc.* **1970**, *92*, 5852.

(38) Faller, J. W.; Anderson, A. S.; Jakubowski, A. *J. Organomet. Chem.* **1971**, *27*, C47.

(39) This value was calculated by assuming that the difference in chemical shifts between the cis and trans carbonyls was 15 ppm, i.e. the same as that found for  $\text{CpMo}(\text{CO})_3\text{X}$ ,<sup>35</sup> and by assuming a frequency factor of  $10^{13}$  in the Arrhenius equation.

(40) Tp rotation in  $\text{TpMo}(\text{CO})_3(\eta^2\text{-C}_3\text{H}_5)$  occurs at +60 °C: Trofimenko, S. *J. Am. Chem. Soc.* **1969**, *91*, 3183.